Hindawi Publishing Corporation
Active and Passive Electronic Components
Volume 2007, Article ID 17692, 7 pages
doi:10.1155/2007/17692

Research Article

The Structural Engineering Strategy for Photonic Material Research and Device Development

Yalin Lu

The Physics Department, Laser and Optics Research Center (LORC), 2354 Fairchild Dr. 2A31, USAF Academy, CO 80840, USA

Received 19 August 2007; Accepted 14 October 2007

Recommended by Min Qiu

A new structural engineering strategy is introduced for optimizing the fabrication of arrayed nanorod materials, optimizing superlattice structures for realizing a strong coupling, and directly developing nanophotonic devices. The strategy can be regarded as "combinatorial" because of the high efficiency in optimizing structures. In this article, this strategy was applied to grow ZnO nanorod arrays, and to develop a new multifunctional photodetector using such nanorod arrays, which is able to simultaneously detect power, energy, and polarization of an incident ultraviolet radiation. The strategy was also used to study the extraordinary dielectric behavior of relaxor ferroelectric lead titanate doped lead magnesium niobate heterophase superlattices in the terahertz frequencies, in order to investigate their dielectric polariton physics and the potential to be integrated with tunable surface resonant plasmonics devices.

1. INTRODUCTION

The combinatorial strategy for materials science and engineering, an experimental concept developed in the 1960s for alloy development and later for new medicine identification, has been reviving in materials science in the recent decade because of the significant advances in material synthesis amethods [1, 2]. In general, a combinatorial strategy includes the development of advanced approaches for both high-throughput material synthesis and efficient parallel characterization of those resulting multicompositional samples [3]. High-throughput syntheses include the fabrication of such combinatorial samples (so-called libraries) using various film deposition methods such as sputtering, pulsed laser deposition (PLD), inkjet delivery, and so forth, and these resulting material libraries can be binary (so-called spreadsheets) or ternary (for simulating a ternary phase diagram), in the format of either "digital" (discrete composition distribution) or "analog" (continuously varying composition). Efficient parallel characterizations require the development of very special tools [4] responding to the property of the research interest, such as structural lattice [5], dielectric constant, luminescence, loss, and so forth, which usually lag behind the high-throughput material synthesis development. Normally, such special tools are required to have capabilities of high-speed scanning and efficient data processing, while the measurement accuracy can still be maintained.

In general, high-throughput syntheses of oxide material libraries are relying on the principle of overlapping thin layers of oxide materials with different compositions as a multilayer under relatively lower synthesis temperature, and a subsequent post-annealing processing on the library will compositionally interdiffuse them into a uniformly solid-state reacted material with either a single-phase or a multiphase structure, depending on their composition stoichiometry. In recent years, this combinatorial principle has been successfully used for rapid discovery of many new materials or fine compositional tuning of oxides including phosphors [6], dielectrics [4], electro-optic materials [7], superconductors [1], and so forth. In Figure 1(a), the schematic for both binary and ternary analog libraries is depicted, which have been mainly used for identifying or fine-tuning the material composition in the past. Figure 1(b) shows the solid state reaction principle through post-annealing processing widely used for making those oxide combinatorial libraries.

Fabrication of a superlattice via alternatively stacking two structurally similar oxide materials offers a unique capability to tailor the property of the research interest via changing its

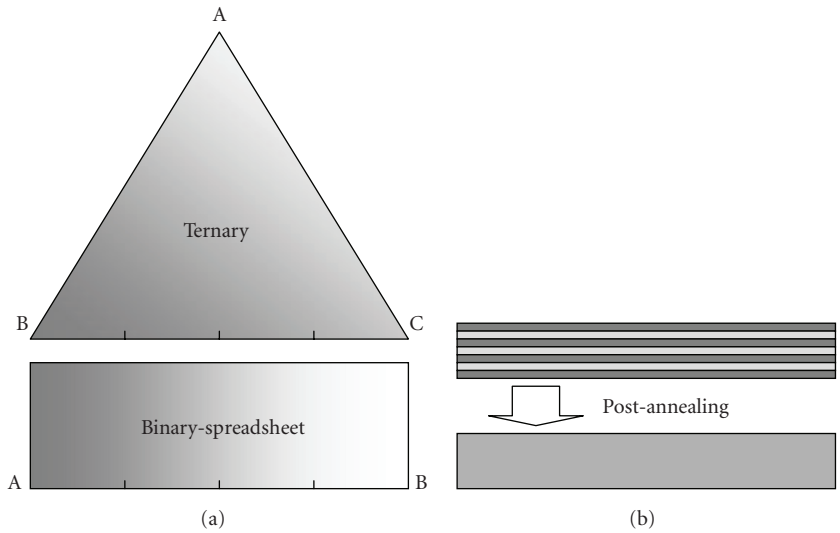

Figure 1: Schematic of ternary (upper) and binary (lower) analog combinatorial libraries (a) and the solid state reaction principle through post-annealing processing the libraries (b).

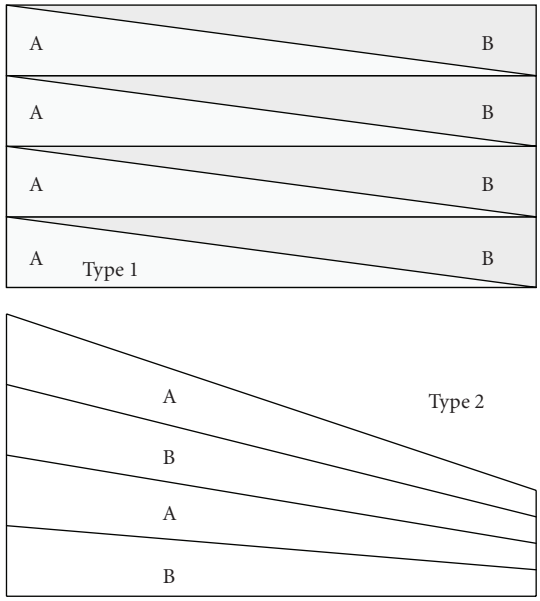

Figure 2: Schematic of two types of structural combinatorial spreadsheets: Type I and type II.

periodicity [8]. Because of the single crystalline structure of a superlattice, frequency-dependent lattice resonances (dispersion of phonons) will occur and will present resonant behaviors at certain frequencies. Such resonant frequencies are mainly determined by the superlattice periodicity and properties of those materials as layers such as piezoelectric coefficients [9]. Interaction of such phonons with incident electromagnetic (EM) radiations (photons) via energy transferring will then result in many new kinds of polaritons, which are responsible for many new and interesting physical phenomena including structurally tailorable band-edge absorption, negative refraction, tunable dielectric constant, nonlinear optics, and so forth. As one of their potential application examples, proper integration of a highly tunable dielectric superlattice with certain nanostructures such as surface resonant plasmonics may realize a large range of frequency tuning in long wavelengths, which will be useful for terahertz (THz) optics.

In this research, such a structural engineering strategy is discussed. It was applied to optimize the growth condition of ZnO nanorod arrays, to develop a new multifunctional UV photodetector using such ZnO nanorod arrays able to simultaneously distinguish power, energy, and polarization of an incident UV light. Furthermore, this strategy was used to study the dispersion behavior of new ferroelectric relaxor lead titanate doped lead magnesium niobate (PMN-PT) heterophase superlattices in the THz frequency range with a goal to investigate some new physical phenomena including the dispersion of the dielectric polaritons and their tunable behaviors. Potential application of such a strategy for negative index materials (NIM) and nonlinear optics are also slightly discussed.

2. THE STRUCTURAL ENGINEERING STRATEGY

The structural engineering strategy is easily applicable to cases where analog binary libraries (spreadsheets) can be fabricated. Key point to implement this strategy will be to keep the as-grown spreadsheet as a superlattice, instead of the previously discussed reacted film. This difference will result in significant challenges in fabrication. For example, post-annealing processing will be omitted in order to suppress the interdiffusion between those adjunct layers if as superlattices. Growth of each superlattice layer through atomic epitaxy is required, and the process should satisfy conditions generally required for a single crystalline epitaxy growth—lattice matching among substrate and two stacking layers, the two layers' similarity in growth characteristics, and so

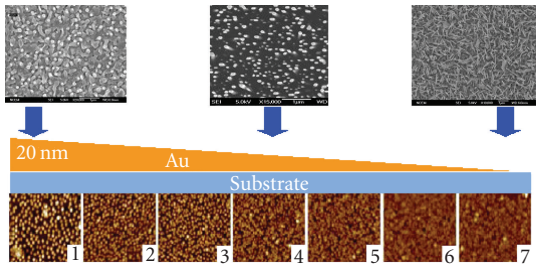

FIGURE 3: The spreadsheet approach used for optimizing the Au catalyst thickness for ZnO nanorod array growth.

forth. Figure 2 shows two possible formats of the analog spreadsheets: each interlayer has a linearly varying composition (Type I) and each interlayer has a linearly varying thickness (Type II). In terminology, if this strategy is used for high-throughput optimization, it can be referred as "structural combinatorial strategy," in comparison to previously mentioned compositional combinatorial strategy. Otherwise, this strategy will remain as the structural engineering strategy.

In this research, the structural engineering strategy will be used to optimize growth condition for fabricating ZnO nanorod arrays. For further making them into imaging photodetectors, ZnO nanorod arrays are required to be vertically aligned with suitable rod size and rod surface density (nanorods per surface area). The Type I structural engineering concept was used to the (Zn,Mg)O material via a pulsed laser deposition (PLD) growth. The fabricated ZnMgO/ZnO/ZnMgO quantum well (QW) spreadsheet will be integrated with a ZnO nanorod array-based photodetector [10] for simultaneously sensing energy, power, and polarization of an incident UV light, without the use of any additional wavelength dispersive components and optical polarization controller. Such new UV photodetectors can find wide applications in biology, environmental protection, and so forth, because of their compactness and cost effectiveness. The Type II strategy was used to the PMN-PT material for realizing heterophase superlattice spreadsheets fabricated by the modified chemical liquid deposition (CLD) approach [11]. "Heterophase" indicates an alternatively stacking of PMN-PT rhombohedral (R) and tetragonal (T) phases, by maintaining their average composition right at the "R" and "T" phases' morphology phase boundary (MPB) [12]. Such superlattices could present minimal interfacial strains and are then suitable for studying their polariton physics and tunable behaviors for long wavelengths.

3. OPTIMIZATION OF ZnO NANOROD ARRAYS

The qualities of ZnO nanorod arrays as potential photodetectors can be evaluated according to nanorod density (nanorods per area), nanorod size, size uniformity, and the degree of their vertical alignment against the substrate, and so forth. The spatial resolution for imaging will be determined by the nanorods' density, size, and uniformity. Good verticality of nanorods is also required to enhance the polar-

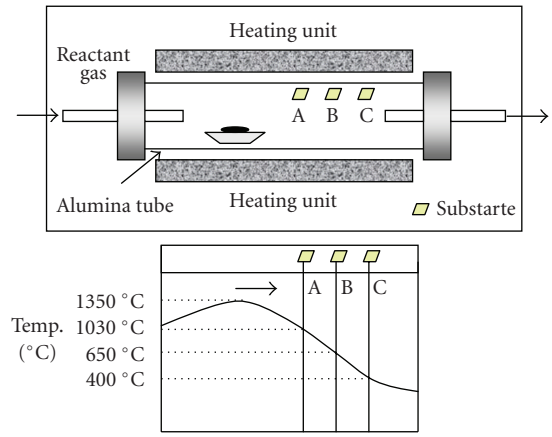

FIGURE 4: Schematic drawing of the CLS growth system with a gradient temperature field.

ization discrimination. In common nanorod growths, phenomena such as spiral growth of nanorods and appearance of nanowires and nanobelts can become very competitive. The growth will be determined by selecting suitable lattice matching, catalyst specie, catalyst thickness, and other processing conditions including growth temperature and catalyst postprocessing. The use of routine trying-error method will be time-consuming and inefficient. However, availability of such a structural engineering approach can solve this issue in a very effective way. In this research, this strategy was used to optimize Au catalyst's thickness, ZnO nanorod growth temperature, and so forth.

The effort to find the best suitable catalyst thickness when using gold (Au) as the catalyst material for growing ZnO nanorod arrays was performed using the (11 $\bar{2}$0) sapphire substrate. An Au thin layer, which has a varying thickness from 0 nm at one end of the spreadsheet to approximately 20 nm at the other end, was sputtered on the sapphire substrate with the help of a moving mask. ZnO nanorod arrays were grown at temperature around 900°C using a standard vapor-liquid-solid (VLS) deposition system. Figure 3 shows the SEM images of the as-grown ZnO nanorod arrays taken from different locations on the spreadsheet. Obviously, dense ZnO nanorod arrays can be obtained when the Au catalyst has a thickness from 5 to 10 nm. When the Au catalyst layer is very thin, it presents typical nanowire growth morphology. Through the use of a thicker Au catalyst layer, the nanorod growth becomes coarser.

Growth temperature optimization of those ZnO nanorods was done using approximately 5 nm thick Au-coated (11 $\bar{2}$0) sapphire wafer in a VLS system having a gradient temperature distribution, as shown in Figure 4. Through identifying the as-grown ZnO nanorods morphology on the wafer via SEM, we found that a suitable growth temperature range from 890 to 950°C. Certain controllability over size and density of ZnO nanorods has been found when selecting a proper growth temperature. Lower growth temperature tends to provide sparser and bigger nanorods. This may be understandable by the nature

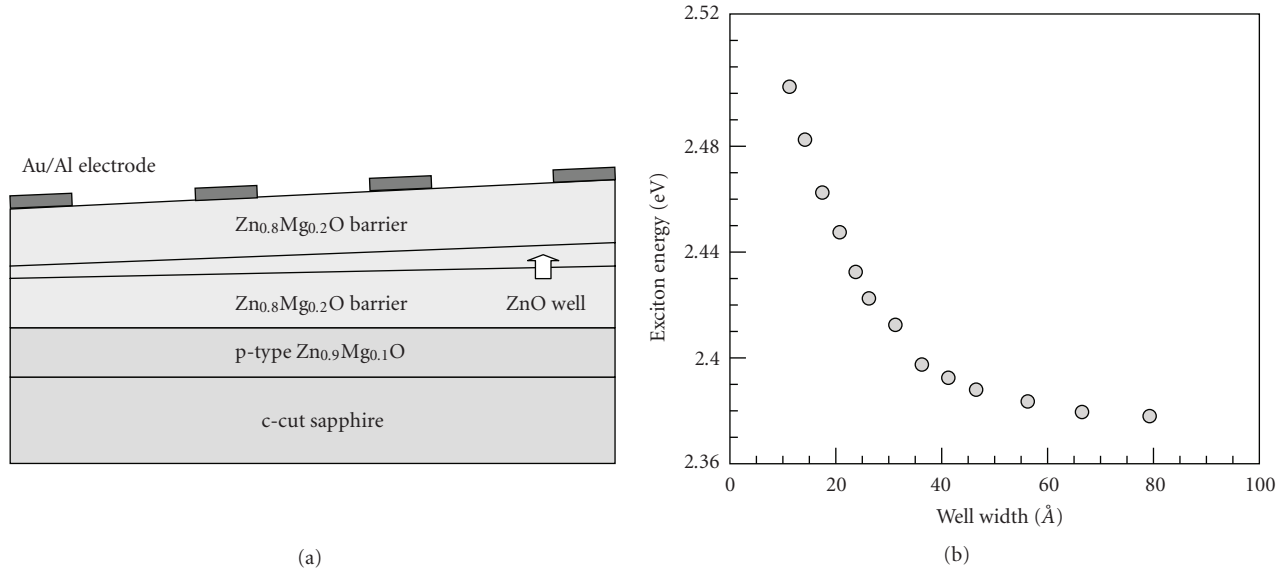

Figure 5: Wavelength distinctive UV photodetectors using a ZnMgO/ZnO/ZnMgO quantum well spreadsheet (a) and the dependence of the exciton energy on the well width (b).

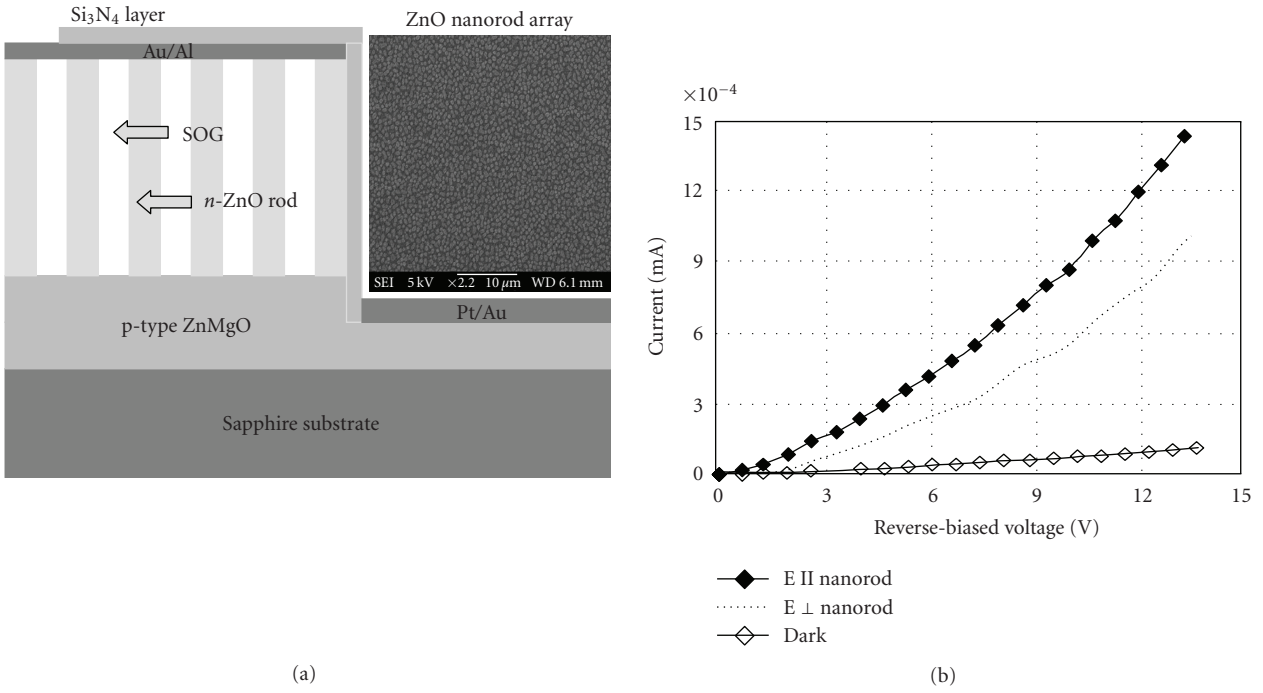

Figure 6: Power and polarization distinctive UV photodetectors using ZnO nanorod arrays grown on the $Zn_{0.9}Mg_{0.1}O$-coated Al_2O_3 (0001) substrate by PLD (a) and typical current-voltage measurements under dark, bright, and different polarizations (b).

of catalyst-assisted ZnO nanorod growth. At the initial stage, Zn vapor dissolves into the Au catalyst to form an alloy droplet. After reaching the saturation, Zn precipitates from the droplet and oxides as the ZnO nanorod grows [13]. During this process, the growth temperature definitely has an impact on Zn partial vapor pressure, its dissolvability into Au, and the degree of saturation, and so forth. Good controllability over nanorods size and density is required for the suggested photodetector to be discussed below, which indicates the necessary of a continuing effort along this research direction.

4. UV PHOTODETECTOR

With a purpose to develop a new type of UV photodetector, which can simultaneously sense power, energy, and

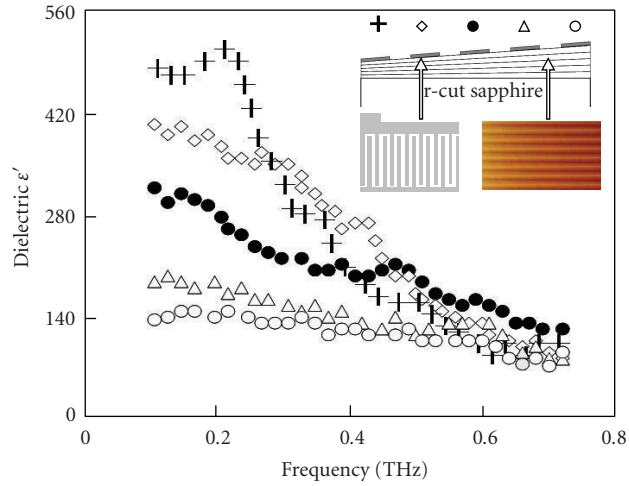

Figure 7: THz dielectric spectra of the PMN-PT heterophase superlattice spreadsheet measured by the time-domain THz measurement technique.

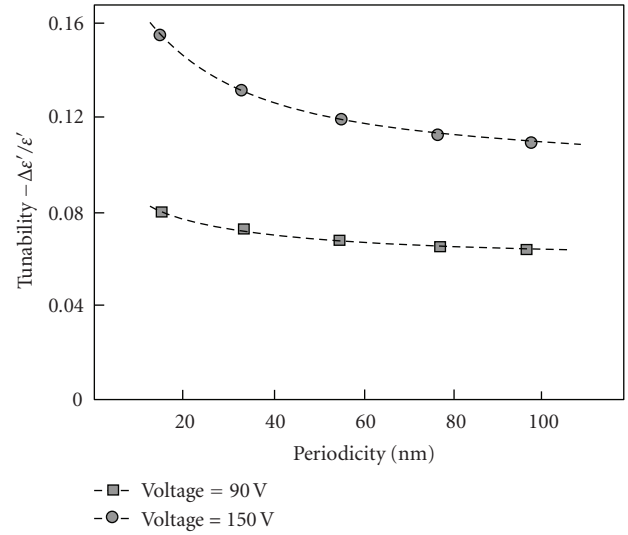

Figure 8: Dielectric tunability of the PMN-PT heterophase superlattice spreadsheet under different applied voltage of 90 V and 150 V, measured at 0.2 THz.

polarization without use of external optical components, a monolithic integration of structurally engineered ZnMgO/ZnO/ZnMgO QW spreadsheet and a well-defined ZnO nanorod array on a p-type $Zn_{0.9}Mg_{0.1}O$-coated c-cut sapphire substrate will be used. As the first part of the photodetector, the spreadsheet is intended for distinguishing wavelength (sensing wavelength). In this part, the p-type $Zn_{0.9}Mg_{0.1}O$ layer is used as a buffer layer for subsequent epitaxial growth via PLD of $Zn_{0.80}Mg_{0.2}O/ZnO/Zn_{0.80}Mg_{0.2}O$ barrier/well/barrier QW spreadsheet, and also as a bottom electrode for making an array of parallel photodetectors, when a linear array of the top Au/Al electrodes was lithographically made (Figure 5(a)). Inside the spreadsheet, both barriers aside the well and the ZnO well maintain a constant thickness ratio of 1.5 : 1, and the ZnO well thickness changes from a few Å at one end of the spreadsheet to over 80 Å at the other. In this case, an incident wavelength can be roughly determined by finding the position of the effective photodetection inside the parallel made photodetector array. Figure 5(b) shows a dependence of ZnO well exciton energy on the well width, which indicates reasonable wavelength detectivity according to the position on the linear detector array responsive to the incident wavelength.

In the second part of the UV photodetector where ZnO nanorod arrays are designed for sensing both optical power and the incident polarization status, the p-type $Zn_{0.9}Mg_{0.1}O$ layer is used to form p-n junctions with those vertically aligned n-type ZnO nanorods grown by the standard vapor-liquid-solid (VLS) deposition (Figure 6(a)), and the growth is catalyzed by a thin layer of sputtered Au (10 nm thick) [14]. Free space among ZnO nanorods was filled by sputtered spin-on-glass (SOG). n-type Au/Al contact was then made on top of ion-etched SOG, and p-type Pt/Au contact was made directly on the bare p-type $Zn_{0.9}Mg_{0.1}O$ aside the ZnO nanorod arrays. Because of the formed nanoscale p-n junctions and each nanorod's large aspect ratio responsive to different polarization statuses [15], this UV photodetector is highly sensitive to the incident UV beam's power and to its polarization status respective to the ZnO nanorod's alignment (Figure 6(b)).

5. PMN-PT HETEROPHASE SUPERLATTICE

In order further to demonstrate the structural engineering strategy's capability, in this section a new complex oxide heterophase superlattice was studied. This new superlattice was found with the potential to have a large dielectric tunability for THz frequencies, because of resonant dielectric polaritons associated with strong coupling between superlattice structure (phonons) and the incident electromagnetic (EM) photons.

A PMN-PT heterophase superlattice spreadsheet was made by linearly varying the dipping speed of a 10 mm wide and 50 mm long r-cut sapphire substrate during the CLD process. The periodicity of the spreadsheet changes from approximately 10 nm at one end to approximately 100 nm at the other, revealed by the SEM cross-section examination. On tope of the spreadsheet, five equally spaced interdigital Ti/Au electrodes (each has an area of $6 \times 6\,mm^2$) were lithographically fabricated (inset in Figure 7). Each interdigital electrode composes of 5 μm wide Ti/Au (25/250 nm) lines separated by 20 μm wide gaps. Dielectric behavior of such superlattices in THz range was measured using the time-domain THz technique [16], in which the transmittance in the time domain is then Fourier-transformed into an absorption spectrum in the frequency domain [17]. By subtracting the substrate's contribution, the net value then represents the anticipated dielectric spectrum. The dielectric tunability was determined by measuring the relative THz electrical field change, $[E_{THz}(V) - E_{THz}(0)]/E_{THz}(0)$, with an applied voltage, $V(t) = V_{max}\sin(2\pi\omega t)$. Here V_{max} is 180 V and ω is 150 Hz. The used THz beam was limited to approximately 1 mm in diameter. All the measurements were locked at 2ω

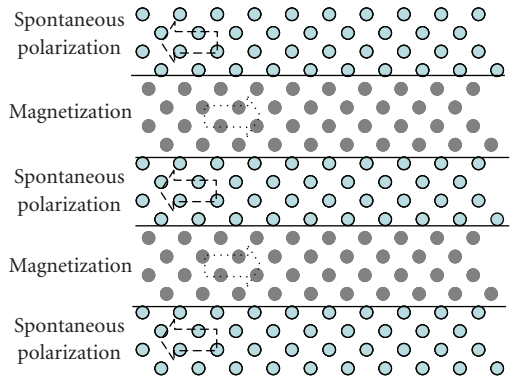

Figure 9: Schematic of the suggested piezoelectric and peizomagnetic (PE/PM) superlattice.

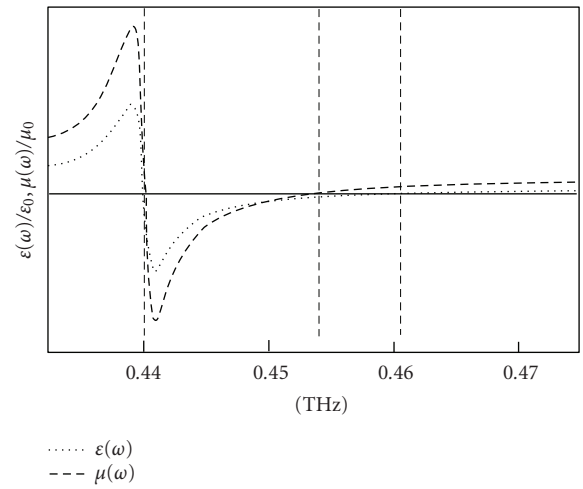

Figure 10: Simulated dielectric spectrum of a PE/PM superlattice in the terahertz frequency range.

by a lock-in amplifier at the room temperature in order to enhance the measurement sensitivity.

Figure 7 shows the THz dielectric spectra of five interdigital electrodes on the spreadsheet. It indicates a significant contribution from both polar nanoclusters relaxation and the variation of mean relaxation frequency respective to the superlattices maximum phase transition temperatures. They are strongly dependent on the interface area per superlattice volume. A small resonance peak can be seen in the spectrum from the superlattice having an average periodicity approximately 60 nm. This represents the existence of dielectric polariton close to one of the sideband resonance frequencies. Dependence of the dielectric tunability on superlattice periodicity under applied voltages of 90 V and 150 V on the spreadsheet measured at 0.2 THz is shown in Figure 8. The results indicate that smaller periodicity and higher voltage are required for achieving a larger tunability. The largest dielectric tunability in the THz frequency range reaches approximately 15%. We believe that this tunability can be further enhanced when the operation is close to the resonance frequency.

6. PIEZOELECTRIC AND PIEZOMAGNETIC SUPERLATTICE

Figure 9 suggests a novel piezoelectric and piezomagnetic (PE/PM) superlattice, in which the interaction between photons and phonons has a possibility to present a frequency range having both permittivity and permeability negative, so-called negative index materials (NIMs) [18]. This frequency range usually occurs immediately after the main resonance band or other sidebands (Figure 10). The structural engineering (combinatorial) strategy can be very useful in locating those resonance frequencies in actual superlattice materials, which are usually hard to be identified because of the lack of knowledge of material parameters of those complex oxides. Without knowing those material parameters with certain accuracies, simulations can only provide very approximated results.

The structural engineering strategy can also be useful for identifying new nonlinear optical (NLO) materials if the structural engineering is simultaneously associated with intentionally ordering the spontaneous polarizations inside ferroelectric materials [19]. This opens up the potential to explore either extraordinarily large optical nonlinearity or new phase matching approach.

7. CONCLUSION

A structural engineering (combinatorial) strategy was introduced, and was used to fabricate highly integrated UV photodetectors with multifunctioning capabilities and to study dielectric polaritons frequency behaviors of PMN-PT heterophase superlattices. Effort in this research not only indicates the high efficiency of the structural engineering (combinatorial) strategy, but also its wide applicability to versatile new research areas of current interests.

ACKNOWLEDGMENT

The author acknowledges the support from the United States Air Force Office of Scientific Research (AFOSR) and the Air Force Research Laboratories (AFRL) at both Wright Patterson and Kirtland.

REFERENCES

[1] X.-D. Xiang, X. Sun, G. Briceño, et al., "A combinatorial approach to materials discovery," *Science*, vol. 268, no. 5218, pp. 1738–1740, 1995.

[2] I. Takeuchi, J. Lauterbach, and M. J. Fasolka, "Combinatorial materials synthesis," *Materials Today*, vol. 8, no. 10, pp. 18–26, 2005.

[3] X.-D. Xiang and I. Takeuchi, *Combinatorial Materials Synthesis*, Marcel Dekker, New York, NY, USA, 2003.

[4] Y. Lu, T. Wei, F. Duewer, et al., "Nondestructive imaging of dielectric-constant profiles and ferroelectric domains with a scanning-tip microwave near-field microscope," *Science*, vol. 276, no. 5321, pp. 2004–2006, 1997.

[5] F. Tsui and Y. S. Chu, "The combinatorial approach: a useful tool for studying epitaxial processes in doped magnetic semiconductors," *Macromolecular Rapid Communications*, vol. 25, no. 1, pp. 189–195, 2004.

[6] J. Wang, Y. Yoo, C. Gao, et al., "Identification of a blue photoluminescent composite material from a combinational library," *Science*, vol. 279, no. 5357, pp. 1712–1714, 1998.

[7] J. Li, F. Duewer, C. Gao, H. Chang, X.-D. Xiang, and Y. Lu, "Electro-optic measurements of the ferroelectric-paraelectric boundary in $Ba_{1-x}Sr_xTiO_3$ materials chips," *Applied Physics Letters*, vol. 76, no. 6, pp. 769–771, 2000.

[8] Y. Lu, "Dielectric and ferroelectric behaviors in $Pb(Mg_{1/3}Nb_{2/3})O_3$-$PbTiO_3$ rhombohedral/tetragonal superlattices," *Applied Physics Letters*, vol. 85, no. 6, pp. 979–981, 2004.

[9] Y.-Q. Lu, Y.-Y. Zhu, Y.-F. Chen, S.-N. Zhu, N.-B. Ming, and Y.-J. Feng, "Optical properties of an ionic-type phononic crystal," *Science*, vol. 284, no. 5421, pp. 1822–1824, 1999.

[10] Y. Lu, I. A. Dajani, and R. J. Knize, "ZnO nanorod arrays as p-n heterojunction ultraviolet photodetectors," *Electronics Letters*, vol. 42, no. 22, pp. 1309–1310, 2006.

[11] Y. Lu, G.-H. Jin, M. Cronin-Golomb, et al., "Fabrication and optical characterization of $Pb(Mg_{1/3}Nb_{2/3})O_3$-$PbTiO_3$ planar thin film optical waveguides," *Applied Physics Letters*, vol. 72, no. 23, pp. 2927–2929, 1998.

[12] Y. Lu and R. J. Knize, "Enhanced dielectric and electro-optic effects in relaxor oxide heterostructured superlattices," *Journal of Physics D*, vol. 37, no. 17, pp. 2432–2436, 2004.

[13] X. Liu, X. Wu, H. Cao, and R. P. H. Chang, "Growth mechanism and properties of ZnO nanorods synthesized by plasma-enhanced chemical vapor deposition," *Journal of Applied Physics*, vol. 95, no. 6, pp. 3141–3147, 2004.

[14] Y. Lu, I. A. Dajani, W. J. Mandeville, R. J. Knize, and S. S. Mao, "New p-n junction photodetector using optimized ZnO nanorod array," *Solid State Phenomena*, vol. 121-123, p. 809, 2006.

[15] Z. Fan, P.-C. Chang, J. G. Lu, et al., "Photoluminescence and polarized photodetection of single ZnO nanowires," *Applied Physics Letters*, vol. 85, no. 25, pp. 6128–6130, 2004.

[16] P. C. M. Planken and H. J. Bakker, "Towards time-resolved THz imaging," *Applied Physics A*, vol. 78, no. 4, pp. 465–469, 2004.

[17] P. Kužel, F. Kadlec, H. Němec, R. Ott, E. Hollmann, and N. Klein, "Dielectric tunability of $SrTiO_3$ thin films in the terahertz range," *Applied Physics Letters*, vol. 88, no. 10, Article ID 102901, 3 pages, 2006.

[18] J. B. Pendry, "Negative refraction makes a perfect lens," *Physical Review Letters*, vol. 85, no. 18, pp. 3966–3969, 2000.

[19] Y. Lu, L. Mao, S.-D. Cheng, N.-B. Ming, and Y.-T. Lu, "Second-harmonic generation of blue light in $LiNbO_3$ crystal with periodic ferroelectric domain structures," *Applied Physics Letters*, vol. 59, no. 5, pp. 516–518, 1991.